

1           **Genomic analysis reveals the influence of climate change and**  
2                           **currents on adaptation in an estuarine species**

3  
4   Ao Li<sup>1,2,3,4,9</sup>, He Dai<sup>5,9</sup>, Ximing Guo<sup>8,9</sup>, Ziyan Zhang<sup>1,6</sup>, Kexin Zhang<sup>1,6</sup>, Chaogang  
5   Wang<sup>1,6</sup>, Wei Wang<sup>1,3,4,7</sup>, Hongju Chen<sup>5</sup>, Xumin Li<sup>5</sup>, Hongkun Zheng<sup>5</sup>, Guofan  
6   Zhang<sup>1,3,4,7\*</sup> and Li Li<sup>1,2,3,4\*</sup>

7  
8   <sup>1</sup>CAS and Shandong Province Key Laboratory of Experimental Marine Biology,  
9   Center for Ocean Mega-Science, Institute of Oceanology, Chinese Academy of  
10   Sciences, Qingdao, China. <sup>2</sup>Laboratory for Marine Fisheries Science and Food  
11   Production Processes, Pilot National Laboratory for Marine Science and Technology,  
12   Qingdao, China. <sup>3</sup>Center for Ocean Mega-Science, Chinese Academy of Sciences,  
13   Qingdao, China. <sup>4</sup>National and Local Joint Engineering Key Laboratory of Ecological  
14   Mariculture, Institute of Oceanology, Chinese Academy of Sciences, Qingdao, China.  
15   <sup>5</sup>Biomarker Technologies Corporation, Beijing, China. <sup>6</sup>University of Chinese  
16   Academy of Sciences, Beijing, China. <sup>7</sup>Laboratory for Marine Biology and  
17   Biotechnology, Pilot National Laboratory for Marine Science and Technology,  
18   Qingdao, China. <sup>8</sup>Haskin Shellfish Research Laboratory, Department of Marine and  
19   Coastal Sciences, Rutgers University, Port Norris, NJ, USA. <sup>9</sup>These authors  
20   contributed equally: A. Li, H. Dai and X. Guo. \*e-mail: [gzhang@qdio.ac.cn](mailto:gzhang@qdio.ac.cn) and  
21   [lili@qdio.ac.cn](mailto:lili@qdio.ac.cn)

22 **Abstract**

23 Understanding the evolutionary forces driving adaptive divergence and identifying the  
24 genomic variations, especially those mediating the plastic responses are critical to  
25 evaluate the adaptive capacity of species upon rapidly changing climate. Here we  
26 report a high-quality genome assembly for an estuarine oyster (*Crassostrea ariakensis*)  
27 and 264 resequenced wild individuals from 11 estuaries along Chinese coastline. This  
28 estuarine oyster evolved decreased polymorphism and a clear population structure  
29 than that of marine species. Historical glaciations, ocean currents and environmental  
30 selection play important role in shaping and maintaining their divergence patterns. We  
31 identified genes, especially for expanded genes *solute carrier family*, showing strong  
32 selective signals and most of them responded to temperature and salinity challenges,  
33 suggesting their significance in environmental adaptation. Higher genetic divergence  
34 of environment-responsive genes especially in upstream intergenic regions potentially  
35 regulate their higher plastic changes, providing genomic basis of plasticity upon  
36 climatic selection. Our findings contribute to assess species' vulnerabilities to  
37 climate-driven decline or extinction.

38 Rapidly changing climate threatens the global biodiversity and geographic  
39 distribution of organisms. Accompanying with the rising of global temperature over  
40 the past decades, the dry regions is getting drier, while wet regions wetter<sup>1</sup>. The  
41 salinity difference is getting greater in estuaries for increasing of salinity in the north  
42 China, while decreasing in the south<sup>2</sup>. Except for environmental selection, species'  
43 distribution patterns are also influenced by stochastic forces including gene flow and  
44 genetic drift. For marine species living in an open area, gene flow is restricted  
45 compared to previous perspectives, and historical climate (like glaciations) and  
46 tectonic events can shift their geographic distributions, as well as the role of the  
47 natural barrier of diluted water<sup>3-7</sup>. Fine-scale local adaptation among different  
48 environmental gradients has been revealed in many marine species, even those with  
49 higher dispersal capacity<sup>8-13</sup>. Evolutionary adaptation to various environments evolves  
50 plastic changes and accumulation of genetic mutations to alter phenotypes reaching  
51 the fitness optimum over generations<sup>14-16</sup>. Most of recent studies independently  
52 revealed the significance of genomic variations<sup>12,17-19</sup> and plasticity<sup>13,20-22</sup> especially  
53 for environmentally responsive genes of marine species in adaptation to changing  
54 ocean environments such as challenges from temperature and salinity disturbances.  
55 Their interaction, genomic variations of environmentally responsive genes/traits, is a  
56 critical predictor of organismal adaptive potential to climate-driven challenges<sup>23,24</sup>.  
57 however, genetic basis of plasticity to environmental heterogeneity remains poorly  
58 understood.

59 Oysters are keystone species in intertidal and estuarine ecology and one of the most  
60 important aquaculture species worldwide. Oyster is sessile species thriving in the  
61 coastal zone with highly environmental variation, and both genetic divergence and  
62 plasticity contribute to its adaptive evolution<sup>11,25-27</sup>, which suggest that the oyster is  
63 excellent model for studying genomic basis of plastic responses to changing climates.  
64 Estuarine oysters (*Crassostrea ariakensis*, Fig. 1a) are broadly distributed in the  
65 estuaries of eastern Asia and experience high extent of environmental gradients in  
66 temperature and salinity<sup>28-30</sup>. A clear genetic structure among different geographic

67 populations by limited neutral markers<sup>28,31-33</sup>, and differentiation in plastic responses  
68 to temperature and salinity stresses between northern and southern populations has  
69 been revealed<sup>2,34</sup>. Understanding whole-genome selective signals and its contribution  
70 to plasticity requires exploring genomic variations and plastic changes together at the  
71 same gene level. Long-read sequencing platforms provide a chromosome-level  
72 assembly and a more informative genome for exploring variations under natural  
73 selection<sup>35-37</sup>. Integrating comparative genomics and genome-wide gene expression  
74 profiles can not only shed light on selective signals by identifying genomic variations  
75 adapted to variable ecotypes, but also provide genomic mechanisms that mediate gene  
76 expression plasticity by identifying genomic variations that located around the  
77 environmental responsive genes<sup>11,12,19</sup>.

78 Here, we sequenced the genome of estuarine oyster *C. ariakensis* and re-sequenced  
79 264 wild oysters collected from 11 sites across most of Chinese estuaries, to reveal its  
80 genetic structure, the potential driven forces and identify genomic regions with  
81 selective signals. Transcriptomes under acute thermal and high-salt stresses, and  
82 reciprocal transplantation were conducted to explore expression patterns of  
83 environmentally responsive genes and further characterized the contribution of  
84 genomic variations at different regions to its gene expression plasticity.

## 85 **Results and Discussion**

86 **Genome assembly and annotation.** To generate a high-quality reference genome, we  
87 sequenced the genome of estuarine oyster *C. ariakensis* using a combination of  
88 short-read and long-read sequencing platforms to generate a contig-level assembly.  
89 Hi-C libraries were also constructed and sequenced to organize them into a  
90 scaffold-level genome assembly. The estimated genome size based on the *k*-mer  
91 distribution analysis was 583.41 Mb (Supplementary Fig. 1, Supplementary Table 1).  
92 The polymorphism level was 0.58%, which was less than half as that of wild marine  
93 oyster species<sup>38</sup> (Pacific oyster *Crassostrea gigas*). and this may be resulted from  
94 limited gene flow of the oyster that are specifically adapted to estuarine environments.  
95 We applied a hierarchical assembly approach using 183.70 Gb of long-reads  
96 (299.24-fold coverage), 64.39 Gb of paired-end reads (104.89-fold coverage) and  
97 106.34 Gb (173.22-fold coverage) of Hi-C data. The final, polished and  
98 high-contiguity genome assembly spans 613.89 Mb comprising 630 contigs with a  
99 contig N50 of 6.97 Mb. Approximately 99.6% of the genome across 416 scaffolds  
100 with a scaffold N50 of 62.26 Mb is presented on 10 linkage groups corresponding to  
101 10 chromosomes of the estuarine oysters (Fig. 1b, Supplementary Table 2). To our  
102 knowledge, this is the most contiguous assembly among bivalve genomes using  
103 long-reads sequencing published to date<sup>35-37</sup>. We mapped pair-end reads to the  
104 assembled genome to assess assembly accuracy, resulting in a 97.93% mapping rate.  
105 The genome assembly captured 92.54% of the Benchmarking Universal Single Copy  
106 Orthologs (BUSCO) datasets (Fig. 1c), indicating a high level of gene region  
107 completeness in the genome assembly. Transcripts from the RNA-seq data were used  
108 to assess gene coverage rate, and 97.15% of the transcripts could be aligned to the  
109 assembly, indicating most of the gene sequences were contained (Supplementary  
110 Table 3). The accuracy of genome sequencing data was 98.32% as determined with  
111 Sanger sequencing (Supplementary Table 4). These results verified that the accuracy  
112 and completeness of the estuarine oyster genome assembly are high and of high  
113 quality at the chromosome scale.

114 We predicted 29,631 protein-coding genes in the estuarine oyster genome combining  
115 gene evidence from homology annotation, *de novo* annotation and transcripts of  
116 mRNA sequencing, and 96.13% of which were functionally annotated  
117 (Supplementary Table 5). Various non-coding RNA sequences were also identified  
118 and annotated in the genome, including 1,077 transfer RNAs, 20 micro RNAs and 131  
119 ribosomal RNAs. A total of 332.40 Mb (54.14%) of repeats and transposable elements  
120 were identified (Supplementary Table 6). Generally, the gene density was inversely  
121 related to the content of repeat elements across all chromosomes.

122

123 **Genome resequencing, variation calling and population structure.** We  
124 resequenced 264 wild oysters of *C. ariakensis* from 11 estuarine areas, representing  
125 the major distribution range across north, middle and south geographical regions of  
126 Chinese coastlines<sup>28,29</sup> (Fig. 2a), and obtained 3.81 Tb clean data. The mapping rate  
127 averaged 95.33% varied from 86.46% to 96.66%, and the effective mapped read depth  
128 averaged 19.89× by aligning reads to the *C. ariakensis* reference genome. We  
129 generated 145,271,754 SNPs (range from 487,881 to 640,962 per individual) and  
130 103,080,822 indels (range from 342,486 to 443,381 per individual) acrossing genes  
131 ranging from 11,383 to 13,321. In addition, we found a considerably lower  
132 polymorphism that averaged 0.47 heterozygous SNPs per Kb per individual  
133 (Supplementary Table 7), which was more than 35-fold lower than that in Pacific  
134 oyster populations<sup>11</sup>. The number of genomic variations including SNPs and indels  
135 (insertions and deletions) was gradually increased from north to south estuarine  
136 oysters, and more than half of variations were SNPs (58.45%) that mainly located at  
137 intergenic regions (57.38%, Supplementary Fig. 2).

138 Genetic structure analysis based on genome-wide SNPs supported previous findings  
139 that differentiations occurred among different geographic populations of *C. ariakensis*  
140 in China, using fitness-related traits, neutral markers and transcriptomic analysis<sup>28,32-34</sup>.  
141 The optimal number of population clusters was identified as  $k = 3$  (Supplementary Fig.  
142 3), exactly representing three main geographic sea areas as north estuaries of China

143 (NEC, 5 sites), middle estuaries of China (MEC, 2 sites) and south estuaries of China  
144 (SEC, 4 sites) (Supplementary Fig. 4). Principle component analysis (PCA),  
145 explaining 15.98% of genetic variance by the two PCs, consistently reveals three  
146 distinct populations of oysters corresponding to NEC, MEC and SEC. A fine-scale  
147 subpopulation was further detected that oysters from Qingdao (QD) site and farther  
148 southern subpopulation (SEC-b) including Taishan (TS) and Qinzhou (QZh) sites  
149 were separated from NEC and SEC, respectively (Fig. 2b). Moreover, Phylogenetic  
150 tree using neighbor-joining (NJ) method supports the above clustering, which first  
151 distinguish the southern population from others and further identified another  
152 subpopulation (NEC-a) within NEC distributed along estuaries of southern Bohai Sea  
153 including oysters from Binzhou (BZ) and Dongying (DY) sites (Fig. 2c). A total of six  
154 subpopulations were identified for 11 wild estuarine sites in China. We calculated the  
155 pairwise  $F_{ST}$  for all polymorphic positions among three populations and QD oysters,  
156 and revealed strong divergence between SEC and other populations, ranged from  
157 0.143 to 0.225 (Fig. 2d), which also detected among oysters from different  
158 geographical sites (Supplementary Table 8). Oysters from MEC and NEC were  
159 clustered together in phylogenetic tree with a lower genetic divergence ( $F_{ST} < 0.05$ ),  
160 which is comparable with the divergence among populations of marine oyster species  
161 in north China<sup>11</sup>. Linkage disequilibrium (LD, measured as  $r^2$ ) decreased to half of its  
162 maximum value range from 2.54 kb to 3.00 kb among three populations of estuarine  
163 oysters (Supplementary Fig. 5), which is substantially slower than marine oyster  
164 species<sup>11</sup>. Our findings provided insights into the fine-scale population structure of  
165 estuarine oysters along the coast of China and revealed the stronger genetic  
166 divergence of southern oysters from others.

167

168 **Limited gene flow, genetic drift and positive selection shape the distribution**  
169 **patterns.** Population structure of estuarine oysters was largely concordant with the  
170 direction of ocean currents especially during the summer, where the northern or  
171 southern coastal currents are not cross over the middle area nearby the Changjiang

172 estuary (Fig. 2a and Supplementary Fig. 6). To investigate the effects of ocean  
173 currents on gene flow, we examined nucleotide diversity ( $\pi$ ) for each population and  
174 found that higher genetic diversity was observed in the middle population ( $3.56 \times 10^{-4}$ )  
175 and QD oysters ( $3.59 \times 10^{-4}$ ) where is the joint of more than one ocean currents, than  
176 that of northern ( $3.33 \times 10^{-4}$ ) and southern ( $3.43 \times 10^{-4}$ ) populations (Fig. 2d) where  
177 only adjoin one ocean current (Fig. 2a and Supplementary Fig. 6). The same pattern  
178 of nucleotide diversity was also confirmed by oysters from individual geographical  
179 sites that oysters from middle sites showed higher  $\pi$  values, while oysters from  
180 northern and southern sites have lower diversity (Fig. 3a), which is contrast to the  
181 terrestrial vertebrates where wildlife harbored higher genetic diversity in southern  
182 China<sup>39</sup>. These findings indicate that ocean currents play important role in shaping  
183 and maintaining genetic structure of *C. ariakensis* in China<sup>11,40</sup>, which contribute to  
184 the homogenization within oyster population by facilitating the mixture of larvae from  
185 sites adjoining the currents with the same direction, but the divergence among  
186 populations adjoining the currents with the different directions such as the NEC and  
187 SEC. However, the MEC oysters showed very limited mixed ancestries from northern  
188 and southern populations (Supplementary Fig. 4), as well as the fine-scale  
189 subpopulations within SEC and NEC even in the same direction of ocean currents  
190 (Fig. 2a), indicating the role of ocean currents in mixing gene pools is restricted as  
191 also found in marine oyster populations<sup>11</sup>. In addition, Changjiang dilute water (CDW)  
192 is considered as a natural barrier that facilitates divergence between north and south  
193 populations of many marine species in China<sup>5-7,41,42</sup>. Here, however, we found that  
194 oysters sampled from the north (NT) and south (SH) part of Changjiang River were  
195 clustered together as MEC, indicating CDW is not the barrier and has limited  
196 influence on distribution and divergence patterns for estuarine oysters where  
197 organisms experience wide-range of salinity disturbance.

198 We employed the pairwise sequentially Markovian coalescent (PSMC) to reconstruct  
199 the demographic history and assess fluctuations in effective population size ( $N_e$ ) of  
200 ancestral estuarine oysters *C. ariakensis* in response to Quaternary climatic change



201 using deep-coverage (25-28×) oyster genomes of two or three individuals from each  
202 of three genetic/geographic populations, as well as three individuals of marine oyster  
203 species from resequencing data with the average coverage of  $20\times^{11}$ . Both of the  
204 marine and estuarine oysters were severely influenced by glaciation events during the  
205 past million years that the  $N_e$  had a peak at ~0.90 mya before the Mindel glaciation  
206 (MG, 0.68~0.80 mya) and then was substantially decreased when subjected to  
207 subsequent three times of glaciations including MG, Riss glaciation (RG, 0.24~0.37  
208 mya) and Würm glaciation (WG, 10,000~120,000 years ago), and a relatively slower  
209 decreasing was found at inter-glaciation period between RG and WG. However, the  
210  $N_e$  of estuarine oyster species was massively lower before historical glaciations and  
211 consistently lower than marine species, and the latter was earlier and more rapidly  
212 increased the population size (Fig. 3b). Moreover, we compared nucleotide diversity  
213 among three populations of estuarine oysters and marine oysters ( $n = 26$ ), and found  
214 that marine species have more than 25-fold higher of  $\pi$  values than that of estuarine  
215 oysters ( $\pi_{C. gigas} = 9.27 \times 10^{-3}$ , Fig. 3c). Similarly, stickleback fishes adapted to  
216 freshwater areas exhibited lower  $\pi$  and  $N_e$  values than counterparts dwelling in  
217 brackish areas<sup>43</sup>. These findings addressed that the specified life history of adaptation  
218 to restricted estuarine areas affected the  $N_e$  and nucleotide diversity of *C. ariakensis*.  
219 Generally, all three oyster populations exhibited similar demographic trajectories until  
220 about 0.2 mya (Fig. 3b). The  $N_e$  curves of southern population was the earliest to split  
221 from others that occurred ~0.18 mya corresponding to the isolation period by the land  
222 bridge between Taiwan and Mainland of China from 0.2 mya to 25,000 years ago<sup>44</sup>.  
223 Accordantly, we calculated the putative range of divergence time was 0.14~0.63 mya  
224 between northern and southern populations of *C. ariakensis* using previously reported  
225 pairwise sequence divergence of *COI* gene<sup>28</sup>, based on the sequence divergence of  
226 *COI* gene<sup>41</sup> and divergence time<sup>45</sup> between *C. gigas* and *C. angulata*. In addition, the  
227 split of  $N_e$  curves between middle and northern populations occurred ~90,000 years  
228 ago, corresponding to the grisly fall of the sea level at the sub-glaciation of WG that  
229 the majority of the Bohai Sea was land<sup>46</sup>. Lower  $N_e$  and nucleotide diversity of

230 northern population (Fig. 3a, b) suggested the stronger recent bottleneck on oysters  
231 dwelling in the Bohai Sea. Decreased nucleotide diversity was also found in Bohai  
232 populations of marine oyster species<sup>11</sup>. The role of bottlenecks and geographic  
233 isolation resulted from historical glaciations and tectonic events in shaping species'  
234 distributions were also demonstrated in other molluscs, such as the divergence  
235 between Atlantic coast and Gulf of Mexico populations of eastern oyster<sup>3</sup>. Our results  
236 not only provide putative divergence times among northern, middle and southern  
237 estuarine oyster populations, but also pointed out historical glaciation and tectonic  
238 event was the critical evolutionary drivers to shape their differentiation.

239 We further characterized the genomic variations related to natural selection among  
240 three oyster populations. The number of SNPs showing heterozygous in northern  
241 oysters but homozygous in southern oysters ( $n = 14,373$ ) were 1.89-fold higher than  
242 those of SNPs showing homozygous in northern oysters but heterozygous in southern  
243 oysters ( $n = 7,595$ ) across 10 chromosomes (Fig. 3d). Correspondingly, homozygous  
244 variations in southern oysters ( $50.71\% \pm 1.92\%$ ) were significantly higher than that in  
245 middle ( $44.35\% \pm 0.39\%$ ) and northern oysters ( $44.53\% \pm 0.86\%$ ) ( $p < 0.01$ ,  
246 Supplementary Fig. 7). Both divergent selection and genetic bottlenecks can result in  
247 purified homogeneous variations. Furthermore, southern oysters ( $35.67\% \pm 0.35\%$ )  
248 evolved significantly higher ratio of genes with non-synonymous alleles than these in  
249 middle ( $33.33\% \pm 0.22\%$ ) and northern ( $31.82\% \pm 0.29\%$ ) oysters ( $p < 0.01$ , Fig. 3e),  
250 suggesting southern oysters were subjected to stronger natural selection. Our results  
251 revealed that stronger natural selection, potentially resulted from strong  
252 environmental gradients, preferred to purify the homozygous mutations in southern  
253 oysters.

254 In summary, genetic bottlenecks from historical glaciations and geographic events  
255 play important role in shaping geographic distribution patterns of estuarine oysters in  
256 China, and gene flow from ocean currents and natural selection from environmental  
257 gradients synergistically contribute to maintain their divergent patterns.

258

259 **Genomic signatures related to environmental adaptation.** Oysters inhabiting in  
260 northern and southern habitats subjected to significant environmental gradients.  
261 Southern habitats are characterized with higher temperature in comparison with  
262 northern and middle habitats. Monthly average sea surface temperature (SST) of six  
263 sampling sites from each of six subpopulations were collected from satellite remote  
264 sensing data during 2000 to 2017. Average SST of southern habitats showed a 10.35 °C  
265 higher than that of northern habitats (Supplementary Fig. 8). In addition, we found a  
266 10.98 ‰ higher of salinity at northern (BZ) site than southern (TS) site<sup>2</sup>. And  
267 increasing ocean salinity contrast would intensify the salinity increases at north  
268 regions but decreases at south regions<sup>47,48</sup>. Thus, variations in temperature and salinity  
269 between northern and southern habitats are two of the critical environmental factors  
270 that driven adaptive divergence of northern and southern oyster populations.  
271 Combining geographically disconnected distribution and limited gene flow, local  
272 adaptation was revealed that southern population evolved higher thermal tolerance  
273 and greater sensitivity to high salinity<sup>2</sup>. Observing distinct population structure among  
274 three oyster populations, we propose that there were genomic regions under selection  
275 contribute to adaptation to higher temperature and lower salinity conditions in the  
276 south.

277 To gain insights into the adaptive genetic basis in adapting to southern environments,  
278 we scanned for selection signatures in two population pairs including a) north vs  
279 south and b) middle vs south. We calculated the fixation index ( $F_{ST}$ ) and selection  
280 statistics (Tajima's  $D$ ) between two population pairs, and used an outlier approach  
281 (top 1%  $F_{ST}$  values,  $F_{ST\_north\ vs.\ south} = 0.693$ ,  $F_{ST\_middle\ vs.\ south} = 0.637$ ) to identify  
282 genomic regions undergoing selective sweeps in these three oyster populations. Only  
283 genomic regions surrounding the selective peaks that overlapped between the two  
284 population pairs, and further located at the ravines of Tajima's  $D$  values along each  
285 chromosome in one of the three populations were considered as selective signals. A  
286 total of 24 selective regions spanning 51 candidate genes (44 annotated) were  
287 identified along chromosomes 2, 3, 4, 6, 8 and 9 among three oyster populations (Fig.

288 4a, b and Supplementary Fig. 9-14, Supplementary Table 9). Most of these candidate  
289 genes in other species have also been reported to respond to different environmental  
290 gradients of salinity and temperature<sup>12,19,49-54</sup>.

291 We conducted RNA-seq analysis to examine the responses of genome-wide and  
292 selective genes using wild oysters, which were exposed to sublethal conditions of  
293 elevated temperature (6 hours under 37 °C) and high-salt (7 days under 60 ‰). Low  
294 expressed genes that the aligned read counts were less than 10 in more than 90%  
295 samples were removed for subsequent analysis. About 44.17% (10,279 of 23,270) and  
296 11.7% (2,757 of 23,650) of highly expressed genes were responsible for high salinity  
297 and temperature stresses respectively, and 1,088 genes were both responsive to the  
298 two stresses (Supplementary Fig. 15). For candidate genes with strong selective  
299 signals, a total of 29 genes were expressed under high salinity and temperature stress  
300 conditions, and 75.9% (22 of 29) and 58.6% (17 of 29) of all expressed genes were  
301 significantly increased or repressed their expression levels ( $p < 0.05$ , Fig. 4c),  
302 indicating genes under selection preferred to respond to these two environmental  
303 changes. Thirteen genes were responsive to both thermal and low salinity stresses,  
304 while three genes were not sensitive to these two stresses. Nine and four genes  
305 specifically responded to high salinity or temperature exposure, respectively. Our  
306 findings reveal that most of genes with strong selective signals were responsible for  
307 adaptation of estuarine oysters to environmental gradients especially for temperature  
308 and salinity.

309

### 310 **Expansion of selective genes contribute to temperature and salinity adaptation.**

311 Among these selective regions, we found two tandem duplications for *Solute carrier*  
312 *family* including 10 copies of *Slc23a2* and four copies of *Monocarboxylate*  
313 *transporter 12* (*Mct12*, also known as *Slc16a12*) (Supplementary Fig. 14c), which  
314 located in the two peaks of chromosome 9 and showed high differentiations among  
315 three oyster populations, where average  $F_{ST}$  values were 0.81 and 0.76 respectively  
316 (Supplementary Fig. 14d). Genomic regions spanning *Slc23a2* gene families exhibited

317 extremely lower Tajima's  $D$  values in northern oysters, while these spanning *Mct12*  
318 gene families had extremely lower Tajima's  $D$  values in southern oysters  
319 (Supplementary Fig. 14e). These findings indicate that *Slc23a2* and *Mct12* genes were  
320 under directional selection at northern and southern environments respectively, and  
321 highlight the critical role of genes belonging to *Slc* families in adaptation of marine  
322 species, such as porpoises and coral, to salinity and temperature gradients<sup>17,19,55,56</sup>.  
323 Moreover, ten copies of *Slc23a2* gene family belong to three orthogroups, where two  
324 of them are annotated as purine permease (a: OG0011985 and c: OG0000489) and  
325 another is annotated as uric acid transporter (OG0000633). Four copies of *Mct12* gene  
326 family belong to one orthogroup annotated as purine efflux pump (OG0000571). All  
327 of these orthogroups were extensively expanded in *C. ariakensis*, as well as in other  
328 two estuarine oysters of *C. virginica* and *C. hongkongensis* in compare with marine  
329 species of *C. gigas* (Supplementary Fig. 16). We found that three copies of *Slc23a2*  
330 genes (*Slc23a2\_a1*, *Slc23a2\_a2* and *Slc23a2\_c2*) in two expanded orthogroups  
331 responded to both temperature and salinity challenges, while three copies of *Mct12*  
332 (*Mct12\_1*, *Mct12\_2* and *Mct12\_3*) genes were responsible for salinity challenges (Fig.  
333 4c). The expanded selective genes of these two gene families responsive to the  
334 temperature and salinity challenges mediates adaptive divergence among different  
335 oyster populations. This finding highlighted the important role of gene duplication,  
336 such as *Heat shock protein (Hsp)* gene family in Pacific oyster dwelling in the  
337 intertidal zones<sup>38,57</sup>, in adapting to species-specifically challenging habitats and  
338 further mediate adaptive divergence among different subspecies or populations<sup>58-61</sup>.

339

340 **Selective preference in upstream intergenic regions of environmentally**  
341 **responsive genes.** We explored the divergence patterns of genomic variations,  
342 including genic and intergenic (upstream and downstream) regions, and expression  
343 responses of these 29 genes under selection to environmental changes by conducting  
344 reciprocal transplant experiments. F<sub>1</sub> progenies bred from each of wild northern and  
345 southern populations were acclimatized at both northern and southern habitats for

346 three months.  $F_{ST}$  were used to quantify the extent of divergence of different genomic  
347 regions and transcriptional changes upon transplantation between two habitats were  
348 used to qualify plastic changes of each selective genes.

349 Expression level of 29 candidate selective genes showed distinct population- and  
350 environment-specific patterns that ten and five genes were highly expressed at  
351 southern and northern oyster populations respectively ( $p < 0.05$ ), while seven and four  
352 genes were highly expressed at northern and southern habitats respectively ( $p < 0.05$ ),  
353 as well as three genes exhibited specifically higher or lower expression at native  
354 habitats ( $p < 0.05$ , Fig. 5a). Environment-specific selective genes correspondingly  
355 exhibited significant higher expression plasticity (19.15%) than that of  
356 population-specific selective genes when oysters were reciprocally transplanted  
357 between northern and southern habitats ( $p = 0.0255$ , Supplementary Fig. 17).

358 We further characterize the divergence of different genomic regions at genome-wide  
359 level, as well as total, population- and environment-specific candidate gene sets. At  
360 genome-wide profile, genic regions showed significantly higher  $F_{ST}$  values (mean  
361  $F_{ST\_genic} = 0.163$ ) than that of intergenic regions ( $F_{ST\_intergenic} = 0.138$ ,  $p < 0.001$ ,  
362 Wilcoxon signed-rank tests, Fig. 5b), indicating genic regions were substantially  
363 preferred to be under selection and evolved higher differentiation between northern  
364 and southern oysters. For all of the 29 candidate genes, both genic ( $F_{ST} = 0.7745$ ) and  
365 intergenic ( $F_{ST} = 0.7585$ ) regions were under strong selection, but no difference was  
366 detected between them ( $p > 0.05$ ). However, at both genic and intergenic regions,  
367 environment-specific genes ( $F_{ST} = 0.7816$ ) evolved significantly higher genomic  
368 divergence than population-specific genes ( $F_{ST} = 0.7274$ ) between northern and  
369 southern oysters ( $p = 0.0230$ , Fig. 5b). Specifically, we found that the upstream  
370 intergenic regions of environment-specific genes exhibited significantly higher  
371 divergence than that of population-specific genes between northern and southern  
372 oysters ( $F_{ST\_environment} = 0.7958$ ,  $F_{ST\_population} = 0.7402$ ,  $p = 0.01512$ ), while there was  
373 no difference of  $F_{ST}$  values at both genic and downstream intergenic regions between  
374 two gene sets ( $p > 0.05$ , Fig. 5c). Further, population-specific genes showed higher

375 divergence at genic region, while environment-specific genes evolved higher  
376 divergence at upstream intergenic region (high divergence at genic region may be  
377 resulted from the higher divergence at upstream intergenic region due to the 100-Kb  
378 sliding window). Although the natural selection preferred to genic regions at  
379 genome-wide level and for population-specific genes, environmentally responsive  
380 genes were preference at upstream intergenic regions and under stronger selection,  
381 which included critical regulatory elements such as promoter and enhancers that  
382 potentially regulate their higher gene expression plasticity<sup>24</sup>. Our findings provide  
383 insights into the genomic basis of plasticity that can evolve and has higher genetic  
384 divergence by natural selection<sup>23,24</sup>, facilitating the assessment of species'  
385 vulnerabilities to climate-driven decline or extinction.

## 386 **Methods**

387 **Genome sequencing.** A wild adult estuarine oyster *Crassostrea ariakensis* was  
388 obtained from the northern China (Binzhou, Bohai Sea, China). Four tissue samples  
389 (gill, mantle, muscle and labial palp) were collected and flash-frozen in the liquid  
390 nitrogen. Genomic DNA extracted from the muscle was used to construct long insert  
391 genomic libraries. Oxford Nanopore Technologies' long-read sequencing platform  
392 generated ~184 Gb of data which corresponding to ~299× coverage. In addition,  
393 libraries with insert size of 350 bp were prepared and sequenced using Illumina HiSeq  
394 4000 platform, which generated ~64 Gb of paired-end reads corresponding to ~105×  
395 coverage of the genome.

396

397 **Genome size and heterozygosity.** Trimmed Illumina short reads were used as input  
398 to calculate the distribution of k-mer copy number (KCN). We selected 21 to obtain  
399 the KCN distribution which showed two distinct peaks (Supplementary Fig. 1). The  
400 first peak (KCN = 45) represents the heterozygous single copy k-mer while the  
401 second peak (KCN = 90) represents the homozygous single copy k-mer in the genome.  
402 Genome size was estimated by the formula  $G = K\_num/peak\ depth$ .

403

404 **Contig-level assembly using long-read data.** The Nanopore long reads, with a read  
405 N50 of 33,230 and a mean read length of 23,240 bp, were used for initial genome  
406 assembly. Error correction of clean data was conducted using Canu<sup>62</sup> v1.5, and then  
407 were assembled using Canu, WTDBG2<sup>63</sup> and SMARTdenovo tools. Quickmerge<sup>64</sup>  
408 v0.2.2 was used to join the three assemblies, and then was corrected for 3 cycles using  
409 long reads by Racon<sup>65</sup> and for 3 cycles using Illumina reads by Pilon<sup>66</sup> v1.22 with  
410 default parameters. The initial assembly of estuarine oyster genome was 613,892,480  
411 bp in length with a contig N50 of 6,967,240 bp.

412

413 **Chromosome-level assembly with Hi-C.** The same genomic DNA extracted from  
414 the muscle was used to construct Illumina library, which was sequenced on the



415 Illumina HiSeq 4000 platform. A total of 106.34 Gb (173.22-fold coverage) of clean  
416 data was obtained, and 41.89% of all reads were truncated that containing enzyme  
417 cutting sites. HiC-Pro<sup>67</sup> was employed to evaluate the alignment efficiency and insert  
418 length distribution for valid interaction pairs (75.51%). Furthermore, the genome  
419 sequence contigs and scaffolds were interrupted in 50 kb length, which were then  
420 sorted and oriented into super scaffolds using LACHESIS<sup>68</sup> with the following  
421 parameters: CLUSTER\_MIN\_RE\_SITES = 47, CLUSTER\_MAX\_LINK\_DENSITY  
422 = 2, CLUSTER\_NONINFORMATIVE\_RATIO = 2,  
423 ORDER\_MIN\_N\_RES\_IN\_TRUN = 40, ORDER\_MIN\_N\_RES\_IN\_SHREDS = 41.  
424

425 **Genome evaluation.** The Hi-C contact heatmap was used to assess the accuracy of  
426 the Hi-C assembly. The density of red color represents the number of Hi-C links  
427 between 100 kb windows on the pseudochromosomes of the final assembly.  
428 Benchmarking Universal Single-Copy Orthologs (BUSCO) v3.0.2 with 978  
429 conserved genes were used to assess the completeness and accuracy of estuarine  
430 oyster genome. The Illumina genomic reads were also aligned to the oyster genome to  
431 assess the completeness using sequence alignment tool BWA<sup>69</sup>.

432  
433 **Repeat annotation.** Transposable elements (TEs) were identified and classified using  
434 homology-based and *de novo*-based approaches. RepeatScout and LTR\_FINDER was  
435 used to construct the *de novo* repeat libraries. The *de novo*-based library was further  
436 classified by PASTEClassifier<sup>70</sup> to obtain a consensus library, and combined with the  
437 repeat library of Repbase data. RepeatMasker<sup>71</sup> v4.0.5 was used to identify TEs in the  
438 estuarine oyster genome with the combined library.

439  
440 **Protein-coding genes annotation.** We adopted three methods including *de*  
441 *novo*-based predictions, homology-based predictions and RNA-seq-based predictions  
442 to annotate the protein-coding genes of estuarine oyster *C. ariakensis*. For the  
443 RNA-seq-based prediction, RNA-seq data generated from four tissues (gill, mantle,

444 muscle and labial palp) using ONT long-reads sequencing platform was filtered to  
445 remove adaptors and then trimmed to remove low-quality bases. Clean reads were  
446 aligned to reference genome using TopHat2<sup>72</sup> and then assembled using Trinity<sup>73</sup>. Full  
447 transcriptome-based genome annotation was predicted using PASA<sup>74</sup> v2.2.2 software.  
448 For the *de novo* prediction, five *ab initio* gene prediction programs, including  
449 Genscan<sup>75</sup> v1.0, Augustus<sup>76</sup> v2.4, GlimmerHMM<sup>77</sup> v3.0.4, GeneID<sup>78</sup> v1.4 and SNAP<sup>79</sup>,  
450 were used to predict genes in the repeat-masked genome. For homolog-based  
451 prediction, the protein sequences of 10 well-annotated species, including *Homo*  
452 *sapiens*, *Danio rerio*, *Aplysia californica*, *Strongylocentrotus purpuratus*, *C. gigas*, *C.*  
453 *virginica*, *Biomphalaria glabrata*, *Lingula anatina*, *Octopus bimaculoides* and  
454 *Mizuhopecten yessoensis*, were downloaded and aligned to the repeat-masked  
455 estuarine oyster genome using tblastn<sup>80</sup> with E-value  $\leq 1E-05$ . We employed  
456 GeMoMa<sup>81</sup> v1.3.1 to predict gene models based on the alignment sequences. Finally,  
457 EvidenceModeler<sup>82</sup> (EVM) v1.1.1 was used to generate a weighted and  
458 non-redundant gene set by integrating all gene models predicted by the above three  
459 methods.

460 Homologous sequences in the genome were identified by genBlastA<sup>83</sup> v1.0.4 using  
461 the integrated gene set, and GeneWise<sup>84</sup> was used to identify pseudogenes. Transfer  
462 RNAs (tRNAs) were defined using tRNAscan-SE<sup>85</sup> v1.3.1 software with eukaryote  
463 default parameters. Micro RNA and Rrna were identified by Infernal BLASTN<sup>86</sup>  
464 against the Rfam<sup>87</sup> database v12.0.

465 Functional annotation of protein-coding genes was conducted by aligning them to the  
466 NCBI non-redundant protein<sup>88</sup> (NR), SwissProt<sup>89</sup>, KOG<sup>90</sup> and TrEMBL<sup>89</sup> databases  
467 using BLAST<sup>86</sup> v2.2.31 with a maximal e-value of 1e-05. Domains were identified  
468 using HMMER<sup>91</sup> v3.0 to search against Pfam<sup>92</sup> databases. Gene set was mapped to  
469 Gene Ontology (GO) terms and KEGG pathway to identify the best match  
470 classification for each gene.

471

472 **Whole-genome resequencing and mapping.** We collected 264 wild oysters of *C.*

473 *ariakensis* from 11 estuarine areas (Fig. 3a), representing the major distribution range  
474 across north, middle and south Chinese coastlines<sup>28,29</sup>. Genomic DNA was isolated  
475 from gill of each oysters following the standard phenol-chloroform extraction  
476 procedure, and then was used to construct a library with an insert size of ~ 350 bp.  
477 Paired-end sequencing libraries were constructed according to the manufacturer's  
478 instructions (Illumina Inc., San Diego, CA, USA) and subsequently sequenced on the  
479 Illumina HiSeq X Ten Sequencer (Illumina Inc.). We obtained ~14.42 Gb of clean  
480 data for each sample, giving an average depth of 19.9× coverage (15-28×)  
481 (Supplementary Table 8). The 150-bp paired-end reads were mapped onto the *C.*  
482 *ariakensis* reference genome (PRJNA715058) with the Burrows-Wheeler Aligner  
483 v.0.7.8<sup>69</sup> using the default parameters (bwa mem -M -t 10 -T 20). Mapping data were  
484 then converted into the BAM format and sorted by SAMtools v.1.3.1<sup>93</sup>, which was  
485 further used to remove duplicate reads. Read pair with the highest mapping quality  
486 was retained if multiple read pairs had identical external coordinates.

487

488 **Genomic variation calling and annotation.** The Genome Analysis Toolkit (GATK)  
489 v.3.7<sup>94</sup> module HaplotypeCaller was used to obtain high-quality variation calling of  
490 each sample. SNPs were further filtered with the parameter 'QD<2.0 || FS>60.0 ||  
491 MQ<40.0'. Similarly, calling of INDELs was conducted and filtered using the  
492 command parameters as 'QD<2.0 || FS>60.0'. Filtered SNPs were annotated by the  
493 SnpEff<sup>95</sup> based on the *C. ariakensis* genome, and then were classified as variations in  
494 regions of exon, intron, splicing sites, and upstream and downstream intergenic  
495 regions, and in types of heterozygous and homozygous variations. To characterize the  
496 types of variations in northern and southern oysters, Plink<sup>96</sup> was used to filter the raw  
497 SNPs of each oyster populations using the parameters of MAF > 0.05 and Int > 0.8.  
498 The same SNPs were retrained and then were singly classified as homozygote or  
499 heterozygote in each oyster population (more than half individuals were the same type  
500 of variation in each oyster population). Variations in exons were further categorized as  
501 synonymous or non-synonymous SNPs. Two-sided two-sample Wilcoxon signed-rank

502 tests were conducted to test whether the ratios of genes with nonsynonymous  
503 variations were different between northern and southern geographic populations,  
504 using the function *wilcoxsign-test* in R package “coin”.

505

506 **Population genetic analysis.** Plink<sup>96</sup> was used to filter the raw SNPs of all  
507 individuals using the parameters of MAF > 0.05 and Int > 0.8. Population structure  
508 was investigated using ADMIXTURE v.1.23<sup>97</sup> with default setting. The number of  
509 assumed genetic clusters  $K$  ranged from 2 to 5, and the optimum number of  $K$  was  
510 assessed by cross-validation (CV) errors. The individual-based neighbor-joining (NJ)  
511 phylogenetic tree was constructed using the MEGA<sup>98</sup> under the Kimura 2-Parameter  
512 model with 1000 bootstraps, and was then visualized using FigTree. We performed  
513 PCA for whole-genome SNPs of all 264 individuals using Eigensoft<sup>99</sup>. To evaluate  
514 linkage disequilibrium decay, the parameter  $r^2$  between any two loci was calculated  
515 within each chromosome using Plink v.1.07<sup>96</sup> with the command (`-ld-window-r2 0`  
516 `-ld-window 99999 -ld-window-kb 500`). The average  $r^2$  values were calculated for  
517 each length of distance and the whole-genome LD was averaged across all  
518 chromosomes. The LD decay plot was depicted against the length of distance.  
519 Popgenome R package<sup>100</sup> was used to calculate Tajima’s  $D$ , global  $F_{ST}$  and nucleotide  
520 diversity ( $\pi$ ) using a 100-kb sliding window with the step size of 10-kb.

521

522 **Demographic history of marine and estuarine oyster species.** We implemented  
523 PMSC<sup>101</sup> to estimate dynamics of effective population size ( $N_e$ ) and the possible  
524 divergence time over the past several million years ago (mya). A total of eight  
525 estuarine oysters (*C. ariakensis*) from northern ( $n = 3$ ), middle ( $n = 2$ ) and ( $n = 3$ )  
526 southern populations and three marine oysters (*C. gigas*)<sup>11</sup> with a high sequencing  
527 depth (*C. ariakensis*: 25~28×, *C. gigas*: ~20×) were used. To alleviate the probability  
528 of false positive, sequencing depth of SNPs was filtered with parameters: MinDepth =  
529 average depth/3, MaxDepth = average depth×2. The PSMC parameters were set as:  
530 `-N25 -t15 -r5 -p '4 + 25*2 + 4 + 6'` to estimate the historical  $N_e$ . The estimated

531 generation time ( $g$ ) was set as 1 for both species, while mutation rates ( $\mu$ ) were  
532 calculated, following the formula  $T_{\text{divergence}} = Ks/2\mu$ , as  $0.3 \times 10^{-8}$  and  $0.2 \times 10^{-8}$  for *C.*  
533 *ariakensis* and *C. gigas*, respectively.

534

535 **Detection of selective signals for adaptation to southern environments.** To identify  
536 candidate selective signals potentially contributing to adaptation of oysters to southern  
537 environments, we calculated two pairs of population fixation statistics ( $F_{ST}$ ) and  
538 selection statistics (Tajima's  $D$ ), including a) north vs south and b) middle vs south, in  
539 a 100-kb sliding window with a step size of 10-kb. Genomic regions showing strong  
540 selective signals were defined as following: 1) regions showed top 1%  $F_{ST}$  values  
541 were overlapped in both comparison pairs; 2) regions located at the ravines of  
542 Tajima's  $D$  values along each chromosome in one of the three oyster populations.

543

544 **Exposure to high temperature and salinity.** To investigate environmental responses  
545 of estuarine oysters to challenges of elevated temperature and high salinity, we  
546 collected wild oysters and acutely exposed to different gradients of temperature of 20 °C  
547 and 37 °C for 6 hours and of salinity of 20 ‰ and 60 ‰ for 7 days, respectively. Gills  
548 from five oysters were individually sampled and immediately flash-frozen in liquid  
549 nitrogen for subsequent RNA-seq analysis.

550

551 **Reciprocal transplantation experiments.** Reciprocal transplantation experiments  
552 were described in our previously study<sup>2</sup>. Briefly, wild oysters derived from northern  
553 (Binzhou: BZ, Bohai Sea) and southern (Taishan: TS, East China Sea) environments  
554 were collected and used to reproduce  $F_1$  generation within population. To potentially  
555 maintain an effective population size, a total of 80 mature male and female oysters  
556 were selected as parental individuals after excluding hermaphrodites by microscopic  
557 examination. Eggs were mixed and then divided into 40 beakers. Sperm from each of  
558 40 male oysters were individually crossed with each beaker of mixed eggs, which  
559 warranted each sperm can fertilized with eggs from different female oysters. Zygotes

560 fathered by eight males were combined into one group. Five groups were reared to the  
561 D-shaped stage and then cultured in one nursery pond during larvae to spat stages.  
562 Two-month-old juvenile oysters from each of two populations were outplanted to two  
563 source habitats to test their responses to reciprocal transplantation. After three months  
564 of acclimation at northern and southern environments, we sampled gills of five  
565 oysters from each of population at both habitats in situ that gills were dissected out  
566 immediately on the boat and flash-frozen in liquid nitrogen for subsequent RNA-seq  
567 analysis.

568

569 **RNA-seq analysis.** Total RNA was isolated from gills sampled from acute stress  
570 experiment (high temperature and salinity) and reciprocal transplant experiment,  
571 using the RNAPrep Pure Tissue Kit (Tiangen) following the manufacturer's protocol.  
572 The RNA integrity and concentration were examined by 1.2% gel electrophoresis and  
573 Nanodrop 2000 spectrophotometer, respectively. DNA contamination was removed  
574 with DNase I treatment. RNA integrity was assessed using the RNA Nano 6000  
575 Assay Kit of the Agilent Bioanalyzer 2100 system. A total amount of 1 µg RNA per  
576 sample was used to construct sequencing libraries using NEBNext Ultra™ RNA  
577 Library Prep Kit, and then were sequenced on an Illumina HiSeq 4000 platform to  
578 generate 150-bp paired-end raw reads. Clean data were obtained by removing reads  
579 containing adapter, reads containing ploy-N and low-quality reads. TopHat2<sup>66</sup> was  
580 used to map clean reads to the estuarine oyster *C. ariakensis* reference genome.  
581 StringTie v2.0 was used for reads assembly. Only reads with a perfect match or one  
582 mismatch were further analyzed and annotated. Gene expression levels were  
583 estimated by fragments per kilobase of transcript per million fragments mapped  
584 (FPKM). We employed DESeq2 to analysis differentially expressed genes (DEGs)  
585 between different populations at northern and southern environments. Genes with an  
586 adjusted *p*-value < 0.01 using the Benjamin and Hochberg's approach were assigned  
587 as DEGs. A hierarchical cluster analysis was performed to indicate expression level of  
588 candidate genes showing strong selective signals, using the *pheatmap* package in R

589 software.

590

591 **Data availability**

592 The genome, whole-genome re-sequencing and transcriptome datasets were deposited  
593 in the Sequence Read Archive (SRA) database under the accession number  
594 PRJNA715058.

595 **Reference**

- 596 1 Chou, C. *et al.* Increase in the range between wet and dry season precipitation. *Nature*  
597 *Geoscience* **6**, 263-267, doi:10.1038/ngeo1744 (2013).
- 598 2 Li, A. *et al.* Molecular and Fitness Data Reveal Local Adaptation of Southern and  
599 Northern Estuarine Oysters (*Crassostrea ariakensis*). *Frontiers in Marine Science* **7**,  
600 doi:10.3389/fmars.2020.589099 (2020).
- 601 3 Buroker, N. E., Hershberger, W. K. & Chew, K. K. Population Genetics of the Family  
602 Ostreidae. II. Interspecific Studies of the Genera *Crassostrea* and *Saccostrea*. *Marine*  
603 *Biology* **54**, 171-184 (1979).
- 604 4 Liu, J. X., Gao, T. X., Wu, S. F. & Zhang, Y. P. Pleistocene isolation in the  
605 Northwestern Pacific marginal seas and limited dispersal in a marine fish, *Chelon*  
606 *haematocheilus* (Temminck & Schlegel, 1845). *Molecular ecology* **16**, 275-288,  
607 doi:10.1111/j.1365-294X.2006.03140.x (2007).
- 608 5 Dong, Y. *et al.* The Impact of Yangtze River Discharge, Ocean Currents and Historical  
609 Events on the Biogeographic Pattern of *Cellana toreuma* along the China Coast. *PLoS*  
610 *ONE* **7**, e36178, doi:10.1371/journal.pone.0036178.g001 (2012).
- 611 6 Ni, G., Li, Q., Kong, L. & Zheng, X. D. Phylogeography of bivalve *Cyclina sinensis*.  
612 testing the historical glaciations and Changjiang River outflow hypotheses in  
613 northwestern Pacific. *PLoS ONE* **7**, e49487, doi:10.1371/journal.pone.0049487.g001  
614 (2012).
- 615 7 Ni, G., Kern, E., Dong, Y. W., Li, Q. & Park, J. K. More than meets the eye: The barrier  
616 effect of the Yangtze River outflow. *Molecular ecology* **26**, 4591-4602,



- 617 doi:10.1111/mec.14235 (2017).
- 618 8 Sanford, E. & Kelly, M. W. Local adaptation in marine invertebrates. *Annual review of*  
619 *marine science* **3**, 509-535, doi:10.1146/annurev-marine-120709-142756 (2011).
- 620 9 Somero, G. N. The physiology of global change: linking patterns to mechanisms.  
621 *Annual review of marine science* **4**, 39-61,  
622 doi:10.1146/annurev-marine-120710-100935 (2012).
- 623 10 Miller, A. D. *et al.* Local and regional scale habitat heterogeneity contribute to genetic  
624 adaptation in a commercially important marine mollusc (*Haliotis rubra*) from  
625 southeastern Australia. *Molecular ecology* **28**, 3053-3072, doi:10.1111/mec.15128  
626 (2019).
- 627 11 Li, L. *et al.* Divergence and plasticity shape adaptive potential of the Pacific oyster. *Nat*  
628 *Ecol Evol* **2**, 1751-1760, doi:10.1038/s41559-018-0668-2 (2018).
- 629 12 Stern, D. B. & Lee, C. E. Evolutionary origins of genomic adaptations in an invasive  
630 copepod. *Nat Ecol Evol* **4**, 1084-1094, doi:10.1038/s41559-020-1201-y (2020).
- 631 13 Kenkel, C. D. & Matz, M. V. Gene expression plasticity as a mechanism of coral  
632 adaptation to a variable environment. *Nature Ecology & Evolution* **1**, 0014,  
633 doi:10.1038/s41559-016-0014 (2016).
- 634 14 Ho, W. C. & Zhang, J. Evolutionary adaptations to new environments generally  
635 reverse plastic phenotypic changes. *Nature communications* **9**, 350,  
636 doi:10.1038/s41467-017-02724-5 (2018).
- 637 15 Gienapp, P., Teplitsky, C., Alho, J. S., Mills, J. A. & Merila, J. Climate change and  
638 evolution: disentangling environmental and genetic responses. *Molecular ecology* **17**,

- 639 167-178, doi:10.1111/j.1365-294X.2007.03413.x (2008).
- 640 16 Pfennig, D. W. *et al.* Phenotypic plasticity's impacts on diversification and speciation.  
641 *Trends in ecology & evolution* **25**, 459-467, doi:10.1016/j.tree.2010.05.006 (2010).
- 642 17 Barrio, A. M. *et al.* The genetic basis for ecological adaptation of the Atlantic herring  
643 revealed by genome sequencing. *eLife* **5**, e12081, doi:10.7554/eLife.12081.001  
644 (2016).
- 645 18 Zong, S. B., Li, Y. L. & Liu, J. X. Genomic architecture of rapid parallel adaptation to  
646 fresh water in a wild fish. *Mol Biol Evol*, doi:10.1093/molbev/msaa290 (2020).
- 647 19 Zhou, X. *et al.* Population genomics of finless porpoises reveal an incipient cetacean  
648 species adapted to freshwater. *Nature communications* **9**, 1276,  
649 doi:10.1038/s41467-018-03722-x (2018).
- 650 20 Sandoval-Castillo, J. *et al.* Adaptation of plasticity to projected maximum temperatures  
651 and across climatically defined bioregions. *Proceedings of the National Academy of*  
652 *Sciences* **117**, 17112-17121, doi:10.1073/pnas.1921124117/-/DCSupplemental  
653 (2020).
- 654 21 Eierman, L. E. & Hare, M. P. Reef-Specific Patterns of Gene Expression Plasticity in  
655 Eastern Oysters (*Crassostrea virginica*). *The Journal of heredity* **107**, 90-100,  
656 doi:10.1093/jhered/esv057 (2016).
- 657 22 Bernal, M. A. *et al.* Species-specific molecular responses of wild coral reef fishes  
658 during a marine heatwave. *Science Advances* **6**, eaay3423 (2020).
- 659 23 Kelly, M. Adaptation to climate change through genetic accommodation and  
660 assimilation of plastic phenotypes. *Philosophical Transactions of the Royal Society B:*

- 661 *Biological Sciences* **374**, 20180176, doi:10.1098/rstb.2018.0176 (2019).
- 662 24 Grishkevich, V. & Yanai, I. The genomic determinants of genotype x environment  
663 interactions in gene expression. *Trends in genetics : TIG* **29**, 479-487,  
664 doi:10.1016/j.tig.2013.05.006 (2013).
- 665 25 Ahlgren, J., Yang, X., Hansson, L. A. & Bronmark, C. Camouflaged or tanned:  
666 plasticity in freshwater snail pigmentation. *Biology Letters* **9**, 20130464-20130464,  
667 doi:10.1098/rsbl.2013.0464 (2013).
- 668 26 Li, A., Li, L., Song, K., Wang, W. & Zhang, G. Temperature, energy metabolism, and  
669 adaptive divergence in two oyster subspecies. *Ecology and evolution* **7**, 6151-6162,  
670 doi:10.1002/ece3.3085 (2017).
- 671 27 Gagnaire, P.-A. *et al.* Analysis of Genome-Wide Differentiation between Native and  
672 Introduced Populations of the Cupped Oysters *Crassostrea gigas* and *Crassostrea*  
673 *angulata*. *Genome biology and evolution* **10**, 2518-2534,  
674 doi:10.12770/dbf64e8d-45dd-437f-b734-00b77606430a10.1093/gbe/evy194 (2018).
- 675 28 Wang, H., Guo, X., Zhang, G. & Zhang, F. Classification of jinjiang oysters  
676 *Crassostrea rivularis* (Gould, 1861) from China, based on morphology and  
677 phylogenetic analysis. *Aquaculture* **242**, 137-155,  
678 doi:10.1016/j.aquaculture.2004.09.014 (2004).
- 679 29 Zhou, M. F. & Allen, S. K. A review of published work on *Crassostrea ariakensis*.  
680 *Journal of Shellfish Research* **22**, 1-20 (2003).
- 681 30 Wang, H. *et al.* Distribution of *Crassostrea ariakensis* in China. *Journal of Shellfish*  
682 *Research* **25**, 789-790 (2006).

- 683 31 Zhang, Q., Allen, S. K., Jr. & Reece, K. S. Genetic variation in wild and hatchery  
684 stocks of Suminoe Oyster (*Crassostrea ariakensis*) assessed by PCR-RFLP and  
685 microsatellite markers. *Marine biotechnology* **7**, 588-599,  
686 doi:10.1007/s10126-004-5105-7 (2005).
- 687 32 Xiao, J., Cordes, J. F., Wang, H., Guo, X. & Reece, K. S. Population genetics of  
688 *Crassostrea ariakensis* in Asia inferred from microsatellite markers. *Marine Biology*  
689 **157**, 1767-1781, doi:10.1007/s00227-010-1449-x (2010).
- 690 33 Kim, W.-J. *et al.* Mitochondrial DNA sequence analysis from multiple gene fragments  
691 reveals genetic heterogeneity of *Crassostrea ariakensis* in East Asia. *Genes Genom.*  
692 **36**, 611-624, doi:10.1007/s13258-014-0198-5 (2014).
- 693 34 Liu, X. *et al.* Transcriptome and Gene Coexpression Network Analyses of Two Wild  
694 Populations Provides Insight into the High-Salinity Adaptation Mechanisms of  
695 *Crassostrea ariakensis*. *Marine biotechnology* **21**, 596-612,  
696 doi:10.1007/s10126-019-09896-9 (2019).
- 697 35 Bai, C. M. *et al.* Chromosomal-level assembly of the blood clam, *Scapharca (Anadara)*  
698 *broughtonii*, using long sequence reads and Hi-C. *GigaScience* **8**,  
699 doi:10.1093/gigascience/giz067 (2019).
- 700 36 Peng, J. *et al.* Chromosome-level analysis of the *Crassostrea hongkongensis* genome  
701 reveals extensive duplication of immune-related genes in bivalves. *Molecular ecology*  
702 *resources* **20**, 980-994, doi:10.1111/1755-0998.13157 (2020).
- 703 37 Song, H. *et al.* The hard clam genome reveals massive expansion and diversification  
704 of inhibitors of apoptosis in *Bivalvia*. *BMC Biol* **19**, 15,

- 705           doi:10.1186/s12915-020-00943-9 (2021).
- 706    38    Zhang, G. *et al.* The oyster genome reveals stress adaptation and complexity of shell  
707           formation. *Nature* **490**, 49-54, doi:10.1038/nature11413 (2012).
- 708    39    Hu, Y. *et al.* Spatial patterns and conservation of genetic and phylogenetic diversity of  
709           wildlife in China. *science advances* **7**, eabd5725, doi:10.1126/sciadv.abd5725 (2021).
- 710    40    Li, C. *et al.* Genome sequences reveal global dispersal routes and suggest convergent  
711           genetic adaptations in seahorse evolution. *Nature communications* **12**, 1094,  
712           doi:10.1038/s41467-021-21379-x (2021).
- 713    41    Wang, H., Qian, L., Liu, X., Zhang, G. & Guo, X. Classification of a common cupped  
714           oyster from southern China. *Journal of Shellfish Research* **29**, 857-866,  
715           doi:10.2983/035.029.0420 (2010).
- 716    42    Wang, H., Zhang, G., Liu, X. & Guo, X. Classification of Common Oysters from North  
717           China. *Journal of Shellfish Research* **27**, 495-503,  
718           doi:10.2983/0730-8000(2008)27[495:COCOFN]2.0.CO (2008).
- 719    43    Raeymaekers, J. A. M. *et al.* Adaptive and non-adaptive divergence in a common  
720           landscape. *Nature communications* **8**, 267, doi:10.1038/s41467-017-00256-6 (2017).
- 721    44    Kimura, M. Paleogeography of the Ryukyu Islands. *Tropics* **10**, 5-24 (2000).
- 722    45    Ren, J., Liu, X., Jiang, F., Guo, X. & Liu, B. Unusual conservation of mitochondrial  
723           gene order in *Crassostrea* oysters: evidence for recent speciation in Asia. *BMC*  
724           *evolutionary biology* **10**, 394, doi:10.1186/1471-2148-10-394 (2010).
- 725    46    Qin, Y., Zhao, Y. & Zhao, S. *Geology of the Bohai Sea*. (Science Press, 1985).
- 726    47    Skirris, N. *et al.* Salinity changes in the World Ocean since 1950 in relation to changing

- 727 surface freshwater fluxes. *Climate Dynamics* **43**, 709-736,  
728 doi:10.1007/s00382-014-2131-7 (2014).
- 729 48 Mekonnen, M. M. & Hoekstra, A. Y. Four billion people facing severe water scarcity.  
730 *Science Advances* **2**, e1500323 (2016).
- 731 49 Ribeiro, C. A., Balestro, F., Grando, V. & Wajner, M. Isovaleric acid reduces Na<sup>+</sup>,  
732 K<sup>+</sup>-ATPase activity in synaptic membranes from cerebral cortex of young rats. *Cellular*  
733 *and molecular neurobiology* **27**, 529-540, doi:10.1007/s10571-007-9143-3 (2007).
- 734 50 Huang, Y., Niwa, J., Sobue, G. & Breitwieser, G. E. Calcium-sensing receptor  
735 ubiquitination and degradation mediated by the E3 ubiquitin ligase dorfins. *The Journal*  
736 *of biological chemistry* **281**, 11610-11617, doi:10.1074/jbc.M513552200 (2006).
- 737 51 Vienken, H. *et al.* Characterization of cholesterol homeostasis in  
738 sphingosine-1-phosphate lyase-deficient fibroblasts reveals a Niemann-Pick disease  
739 type C-like phenotype with enhanced lysosomal Ca<sup>2+</sup> storage. *Scientific reports* **7**,  
740 43575, doi:10.1038/srep43575 (2017).
- 741 52 Pagano, M. *et al.* Insights into the residence in lipid rafts of adenylyl cyclase AC8 and  
742 its regulation by capacitative calcium entry. *Am J Physiol Cell Physiol* **296**,  
743 C607–C619, doi:10.1152/ajpcell.00488.2008.-Adenylyl (2009).
- 744 53 Weinman, E. J., Dubinsky, W. P. & Shenolikar, S. Reconstitution of cAMP-Dependent  
745 Protein Kinase Regulated Renal Na<sup>+</sup>-H<sup>+</sup> Exchanger. *J. Membr. Biol.* **101**, 11-18  
746 (1988).
- 747 54 Fonteles, M. C., Greenberg, R. N., Monteiro, H. S. A., Currie, M. G. & Forte, L. R.  
748 Natriuretic and kaliuretic activities of guanylin and uroguanylin in the isolated perfused

- 749 rat kidney. *The American Journal of Physiology* **F191-F197** (1998).
- 750 55 Kenkel, C. D., Meyer, E. & Matz, M. V. Gene expression under chronic heat stress in  
751 populations of the mustard hill coral (*Porites astreoides*) from different thermal  
752 environments. *Molecular ecology* **22**, 4322-4334, doi:10.1111/mec.12390 (2013).
- 753 56 Hoglund, P. J., Nordstrom, K. J., Schioth, H. B. & Fredriksson, R. The solute carrier  
754 families have a remarkably long evolutionary history with the majority of the human  
755 families present before divergence of Bilaterian species. *Mol Biol Evol* **28**, 1531-1541,  
756 doi:10.1093/molbev/msq350 (2011).
- 757 57 Guo, X., He, Y., Zhang, L., Lelong, C. & Jouaux, A. Immune and stress responses in  
758 oysters with insights on adaptation. *Fish & shellfish immunology* **46**, 107-119,  
759 doi:10.1016/j.fsi.2015.05.018 (2015).
- 760 58 Li, A., Li, L., Wang, W., Song, K. & Zhang, G. Transcriptomics and Fitness Data  
761 Reveal Adaptive Plasticity of Thermal Tolerance in Oysters Inhabiting Different Tidal  
762 Zones. *Front Physiol* **9**, 825, doi:10.3389/fphys.2018.00825 (2018).
- 763 59 Zhang, G. *et al.* Molecular Basis for Adaptation of Oysters to Stressful Marine  
764 Intertidal Environments. *Annual review of animal biosciences* **4**, 357-381,  
765 doi:10.1146/annurev-animal-022114-110903 (2016).
- 766 60 Li, A., Li, L., Wang, W. & Zhang, G. Evolutionary trade-offs between baseline and  
767 plastic gene expression in two congeneric oyster species. *Biology Letters* **15**,  
768 20190202, doi:10.1098/rsbl.2019.0202 (2019).
- 769 61 Ghaffari, H., Wang, W., Li, A., Zhang, G. & Li, L. Thermotolerance Divergence  
770 Revealed by the Physiological and Molecular Responses in Two Oyster Subspecies of

- 771 Crassostrea gigas in China. *Front Physiol* **10**, 1137, doi:10.3389/fphys.2019.01137  
772 (2019).
- 773 62 Koren, S. *et al.* Canu: scalable and accurate long-read assembly via adaptive k-mer  
774 weighting and repeat separation. *Genome research* **27**, 722-736,  
775 doi:10.1101/gr.215087.116 (2017).
- 776 63 Jayakumar, V. & Sakakibara, Y. Comprehensive evaluation of non-hybrid genome  
777 assembly tools for third-generation PacBio long-read sequence data. *Briefings in*  
778 *bioinformatics* **20**, 866-876, doi:10.1093/bib/bbx147 (2019).
- 779 64 Chakraborty, M., Baldwin-Brown, J. G., Long, A. D. & Emerson, J. J. Contiguous and  
780 accurate de novo assembly of metazoan genomes with modest long read coverage.  
781 *Nucleic acids research* **44**, e147, doi:10.1093/nar/gkw654 (2016).
- 782 65 Vaser, R., Sovic, I., Nagarajan, N. & Sikic, M. Fast and accurate de novo genome  
783 assembly from long uncorrected reads. *Genome research* **27**, 737-746,  
784 doi:10.1101/gr.214270.116 (2017).
- 785 66 Walker, B. J. *et al.* Pilon: An Integrated Tool for Comprehensive Microbial Variant  
786 Detection and Genome Assembly Improvement. *PLoS ONE* **9**, e112963,  
787 doi:10.1371/journal.pone.0112963.g001 (2014).
- 788 67 Servant, N. *et al.* HiC-Pro: an optimized and flexible pipeline for Hi-C data processing.  
789 *Genome biology* **16**, 259, doi:10.1186/s13059-015-0831-x (2015).
- 790 68 Burton, J. N. *et al.* Chromosome-scale scaffolding of de novo genome assemblies  
791 based on chromatin interactions. *Nature biotechnology* **31**, 1119-1125,  
792 doi:10.1038/nbt.2727 (2013).



- 793 69 Li, H. & Durbin, R. Fast and accurate short read alignment with Burrows-Wheeler  
794 transform. *Bioinformatics* **25**, 1754-1760, doi:10.1093/bioinformatics/btp324 (2009).
- 795 70 Hoede, C. *et al.* PASTEC: An Automatic Transposable Element Classification Tool.  
796 *PLoS ONE* **9**, e91929, doi:10.1371/journal.pone.0091929.t001 (2014).
- 797 71 Tarailo-Graovac, M. & Chen, N. Using RepeatMasker to identify repetitive elements in  
798 genomic sequences. *Curr Protoc Bioinformatics* **Chapter 4**, Unit 4 10,  
799 doi:10.1002/0471250953.bi0410s25 (2009).
- 800 72 Kim, D. *et al.* TopHat2: accurate alignment of transcriptomes in the presence of  
801 insertions, deletions and gene fusions. *Genome biology* **14**, R36 (2013).
- 802 73 Grabherr, M. G. *et al.* Full-length transcriptome assembly from RNA-Seq data without  
803 a reference genome. *Nature biotechnology* **29**, 644-652, doi:10.1038/nbt.1883 (2011).
- 804 74 Campbell, M. A., Haas, B. J., Hamilton, J. P., Mount, S. M. & Buell, C. R.  
805 Comprehensive analysis of alternative splicing in rice and comparative analyses with  
806 *Arabidopsis*. *BMC genomics* **7**, 327, doi:10.1186/1471-2164-7-327 (2006).
- 807 75 Burge, C. & Karlin, S. Prediction of complete gene structures in human genomic DNA.  
808 *Journal of molecular biology* **268**, 78-94 (1997).
- 809 76 Stanke, M. & Waack, S. Gene prediction with a hidden Markov model and a new intron  
810 submodel. *Bioinformatics* **19 Suppl 2**, ii215-225, doi:10.1093/bioinformatics/btg1080  
811 (2003).
- 812 77 Majoros, W. H., Pertea, M. & Salzberg, S. L. TigrScan and GlimmerHMM: two open  
813 source ab initio eukaryotic gene-finders. *Bioinformatics* **20**, 2878-2879,  
814 doi:10.1093/bioinformatics/bth315 (2004).

- 815 78 Alioto, T., Blanco, E., Parra, G. & Guigo, R. Using geneid to Identify Genes. *Curr*  
816 *Protoc Bioinformatics* **64**, e56, doi:10.1002/cpbi.56 (2018).
- 817 79 Korf, I. Gene finding in novel genomes. *Bmc Bioinformatics* **5**, 59 (2004).
- 818 80 Altschul, S. F. *et al.* Gapped BLAST and PSI-BLAST: a new generation of protein  
819 database search programs. *Nucleic acids research* **25**, 3389-3402 (1997).
- 820 81 Keilwagen, J., Hartung, F., Paulini, M., Twardziok, S. O. & Grau, J. Combining  
821 RNA-seq data and homology-based gene prediction for plants, animals and fungi.  
822 *Bmc Bioinformatics* **19**, 189, doi:10.1186/s12859-018-2203-5 (2018).
- 823 82 Haas, B. J. *et al.* Automated eukaryotic gene structure annotation using  
824 EVIDENCEModeler and the Program to Assemble Spliced Alignments. *Genome biology*  
825 **9**, R7, doi:10.1186/gb-2008-9-1-r7 (2008).
- 826 83 She, R., Chu, J. S., Wang, K., Pei, J. & Chen, N. GenBlastA: enabling BLAST to  
827 identify homologous gene sequences. *Genome research* **19**, 143-149,  
828 doi:10.1101/gr.082081.108 (2009).
- 829 84 Birney, E., Clamp, M. & Durbin, R. GeneWise and Genomewise. *Genome research* **14**,  
830 doi:10.1101/ (2004).
- 831 85 Lowe, T. M. & Eddy, S. R. tRNAscan-SE: a program for improved detection of transfer  
832 RNA genes in genomic sequence. *Nucleic acids research* **25**, 955-964 (1997).
- 833 86 Altschul, S. F., Gish, W., Miller, W., Myers, E. W. & Lipman, D. J. Basic Local  
834 Alignment Search Tool. *Journal of molecular biology* **215**, 403-410 (1990).
- 835 87 Griffiths-Jones, S. *et al.* Rfam: annotating non-coding RNAs in complete genomes.  
836 *Nucleic acids research* **33**, D121-124, doi:10.1093/nar/gki081 (2005).

- 837 88 Marchler-Bauer, A. *et al.* CDD: a Conserved Domain Database for the functional  
838 annotation of proteins. *Nucleic acids research* **39**, D225-229,  
839 doi:10.1093/nar/gkq1189 (2011).
- 840 89 Boeckmann, B. *et al.* The SWISS-PROT protein knowledgebase and its supplement  
841 TrEMBL in 2003. *Nucleic acids research* **31**, 365-370, doi:10.1093/nar/gkg095 (2003).
- 842 90 Tatusov, R. L. *et al.* The COG database: new developments in phylogenetic  
843 classification of proteins from complete genomes. *Nucleic acids research* **29**, 22-28  
844 (2001).
- 845 91 Mistry, J., Finn, R. D., Eddy, S. R., Bateman, A. & Punta, M. Challenges in homology  
846 search: HMMER3 and convergent evolution of coiled-coil regions. *Nucleic acids*  
847 *research* **41**, e121, doi:10.1093/nar/gkt263 (2013).
- 848 92 Finn, R. D. *et al.* Pfam: clans, web tools and services. *Nucleic acids research* **34**,  
849 D247-251, doi:10.1093/nar/gkj149 (2006).
- 850 93 Li, H. *et al.* The Sequence Alignment/Map format and SAMtools. *Bioinformatics* **25**,  
851 2078-2079, doi:10.1093/bioinformatics/btp352 (2009).
- 852 94 McKenna, A. *et al.* The Genome Analysis Toolkit: a MapReduce framework for  
853 analyzing next-generation DNA sequencing data. *Genome research* **20**, 1297-1303,  
854 doi:10.1101/gr.107524.110 (2010).
- 855 95 Cingolani, P. *et al.* A program for annotating and predicting the effects of single  
856 nucleotide polymorphisms, SnpEff: SNPs in the genome of *Drosophila melanogaster*  
857 strain w1118; iso-2; iso-3. *Fly* **6**, 80-92, doi:10.4161/fly.19695 (2012).
- 858 96 Purcell, S. *et al.* PLINK: a tool set for whole-genome association and population-based

859 linkage analyses. *American journal of human genetics* **81**, 559-575,  
860 doi:10.1086/519795 (2007).

861 97 Alexander, D. H., Novembre, J. & Lange, K. Fast model-based estimation of ancestry  
862 in unrelated individuals. *Genome research* **19**, 1655-1664, doi:10.1101/gr.094052.109  
863 (2009).

864 98 Kumar, S., Stecher, G., Li, M., Knyaz, C. & Tamura, K. MEGA X: Molecular  
865 Evolutionary Genetics Analysis across Computing Platforms. *Mol Biol Evol* **35**,  
866 1547-1549, doi:10.1093/molbev/msy096 (2018).

867 99 Price, A. L. *et al.* Principal components analysis corrects for stratification in  
868 genome-wide association studies. *Nature genetics* **38**, 904-909, doi:10.1038/ng1847  
869 (2006).

870 100 Pfeifer, B., Wittelsburger, U., Ramos-Onsins, S. E. & Lercher, M. J. PopGenome: an  
871 efficient Swiss army knife for population genomic analyses in R. *Mol Biol Evol* **31**,  
872 1929-1936, doi:10.1093/molbev/msu136 (2014).

873 101 Li, H. & Durbin, R. Inference of human population history from individual  
874 whole-genome sequences. *Nature* **475**, 493-496, doi:10.1038/nature10231 (2011).  
875

876 **Acknowledgements**

877 L.L. is supported by the National Key R&D Program of China (No.  
878 2018YFD0900304) and the Strategic Priority Research Program of the Chinese  
879 Academy of Sciences (No. XDA23050402). A.L. is supported by the Distinguished  
880 Young Scientists Research Fund of Key Laboratory of Experimental Marine Biology,  
881 Chinese Academy of Sciences (No. KLEMB-DYS04) and by China Postdoctoral  
882 Science Foundation (No. 2019TQ0324). A.L. and L.L. are supported by Key  
883 Deployment Project of Centre for Ocean Mega-Research of Science, Chinese  
884 Academy of Sciences (No. COMS2019Q06). L.L. is also supported by the National  
885 Natural Science Foundation of China (No. 31572620) and the Technology and the  
886 Modern Agro-industry Technology Research System (No. CARS-49). We thank X.  
887 Wang, Z. Jia, Z. She, Y. Zhang, Z. Yu, W. Quan, Z. Zeng and Y. Ning for sampling  
888 collection, and B. Yin and J. Qi for information on marine currents.

889

890 **Author contributions**

891 L.L., G.Z. and X.G. conceived the study and participated in final data analysis,  
892 interpretation and drafting the manuscript. A.L. carried out the data analysis and  
893 drafted the manuscript. H.D., A.L., H.C., X.L. and H.Z. contributed to the selective  
894 sweep analysis. A.L., Z.Z., K.Z. and C.W. collected and sampled oyster specimens.  
895 A.L. and W.W. produced the F<sub>1</sub> progeny. A.L., L.L., X.G. and G.Z. revised the  
896 manuscript. All authors approved the manuscript for publication. The authors declare  
897 no competing interests.

898

899 **Competing interests**

900 The authors declare no competing interests.

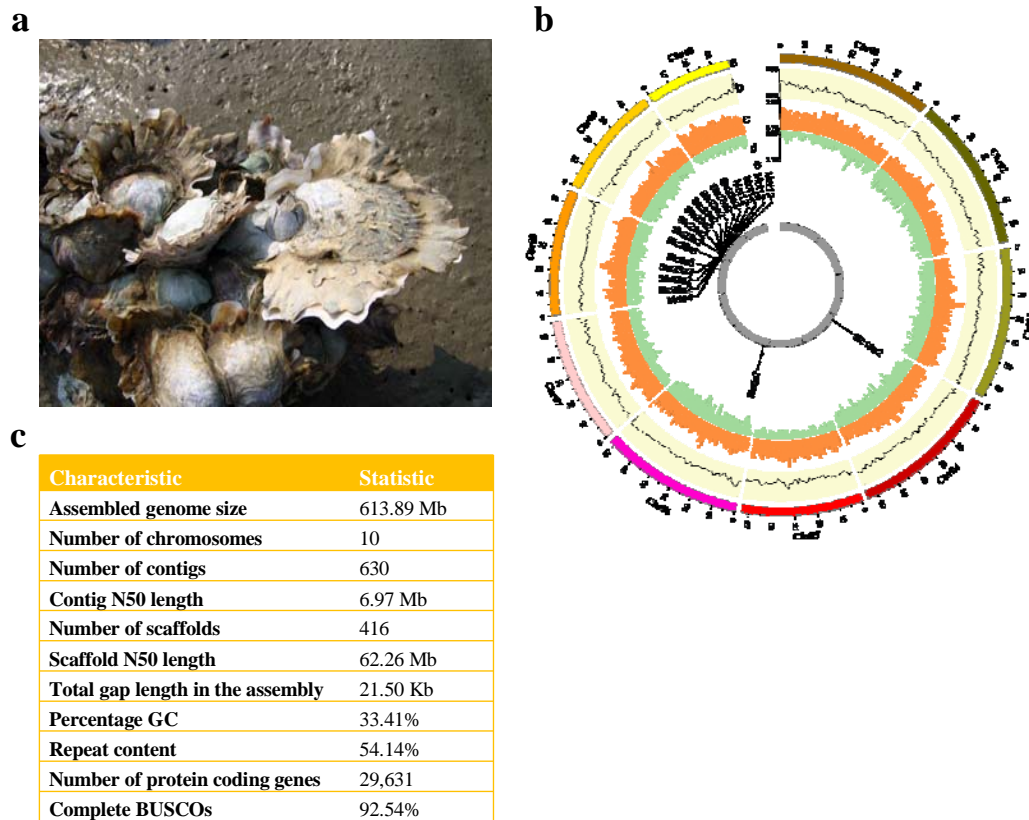


**Fig. 1 | High-quality assembly of the genome of estuarine oyster *Crassostrea ariakensis*.** **a**, Estuarine oyster (photograph by Lumin Qian). **b**, CIRCOS plot showing the distribution of GC content, transposable elements (TE), coding sequences (CDS) and candidate genes (*solute carrier families*) surrounding selective sweep signals (see **Fig. 4**) in each chromosome of the *C. ariakensis* genome. **c**, Summary of the *C. ariakensis* genome assembly and gene annotation statistics.

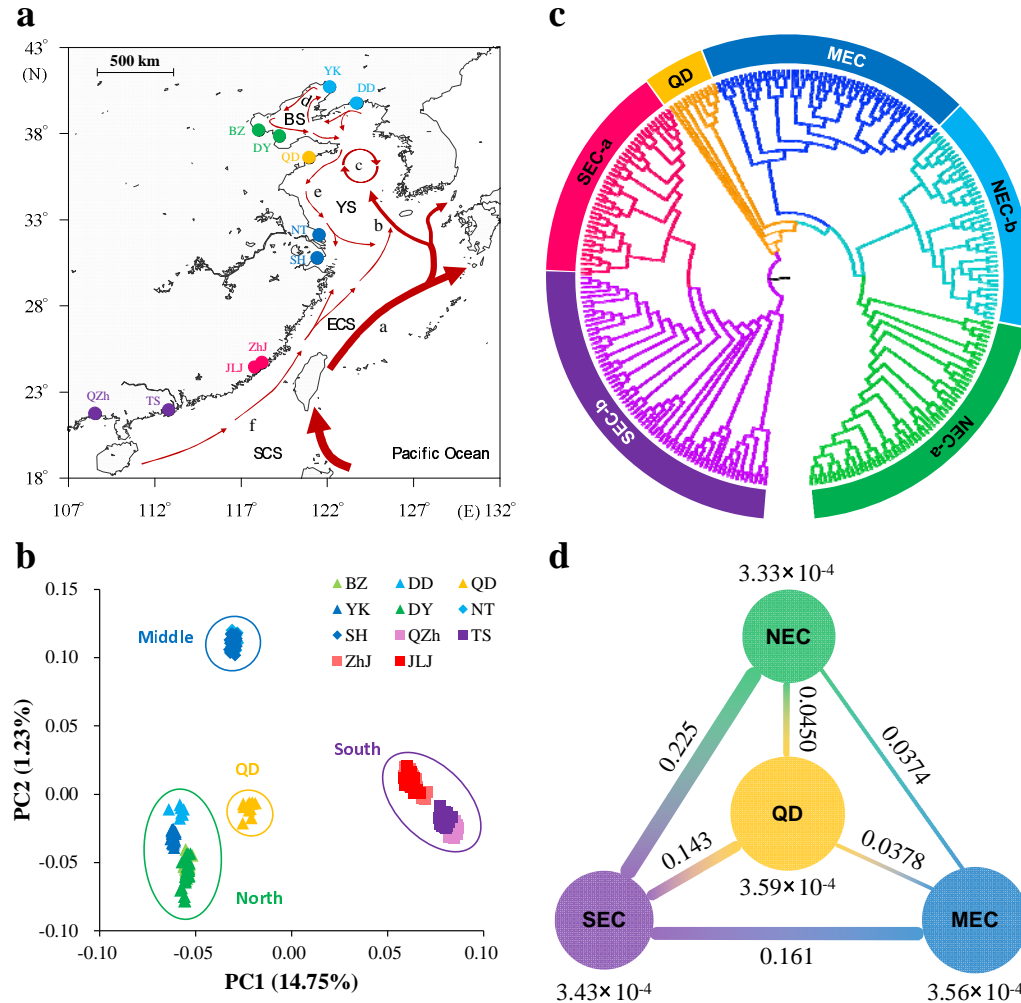


**Fig. 2 | Geographic distribution and genetic structure of the *Crassostrea ariakensis* across the estuaries of China. **a**, Sampling locations of 264 wild estuarine oysters across 11 estuaries in China. The red and arrowed curves represent ocean currents in summer. **a**: Kuroshio current, **b**: Yellow Sea Warm Current, **c**: Yellow Sea Cold Water Mass, **d**: Bohai Sea Circulation, **e**: China Coastal Current, **f**: South China Sea Warm Current. SCS: South China Sea, ECS: East China Sea, YS: Yellow Sea, BS: Bohai Sea. DD: Dandong, YK: Yingkou, BZ: Binzhou, DY: Dongying, QD: Qingdao, NT: Nantong, SH: Shanghai, JLJ: Jiulongjiang, ZhJ: Zhangjiang, TS: Taishan, QZh: Qinzhou. **b**, Plots of principal components 1 and 2 of the 264 oyster individuals. **c**, Phylogenetic tree of estuarine oysters inferred from whole-genome SNPs by the neighbour-joining (NJ) method. NEC-a: north estuaries of China, including BZ and DY, NEC-b: DD and YK, MEC: middle estuaries of China, including NT and SH, SEC-a: south estuaries of China, including JLJ and ZhJ, and SEC-b: TS and QZh. **d**, Nucleotide diversity and genetic divergence across the four populations. The value under the circle is nucleotide diversity ( $\pi$ ) for the oyster population, and values between population pairs indicate genetic divergence ( $F_{ST}$ ).**

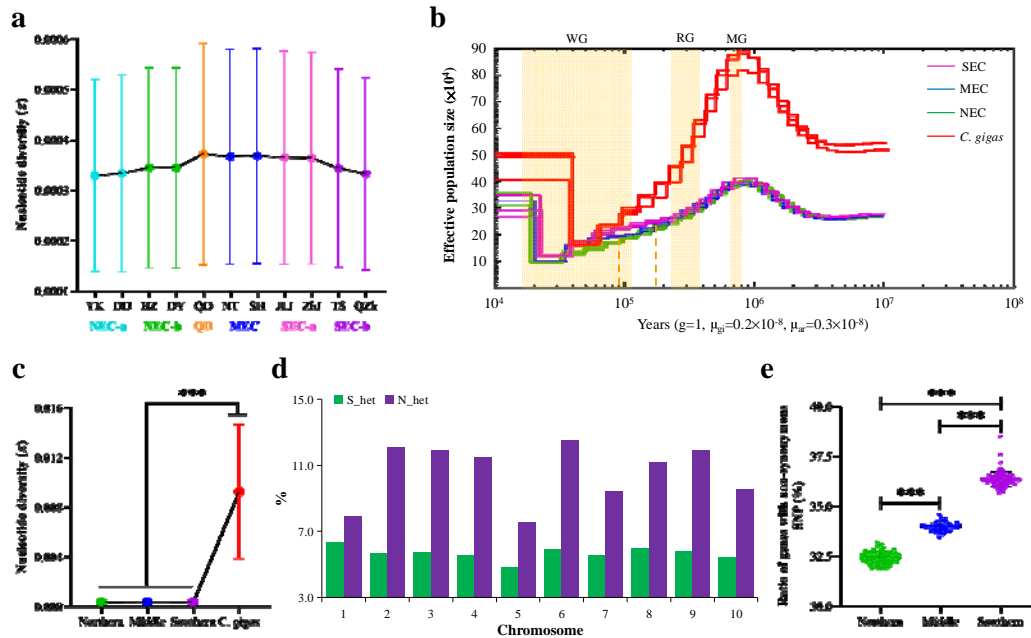


**Fig. 3 | Effects of gene flow, historical glaciation and natural selection on population structure of *C. ariakensis*.** **a**, Nucleotide diversity ( $\pi$ ) of 11 oyster populations of *C. ariakensis*. **b**, Demographic histories of marine oyster species *C. gigas* (gi) and estuarine oyster species *C. ariakensis* (ar) including southern, middle and northern populations (SEC, MEC and NEC), inferred by the PSMC model. The period of the Mindel glaciation (MG, 0.68~0.80 mya), Riss glaciation (MG, 0.24~0.37 mya) and Würm glaciation (WG, 10,000~120,000 years ago) were shaded by pink. **c**, The ratios of SNPs showing heterozygous in northern oysters but homozygous in southern oysters (N\_het) and those of SNPs showing homozygous in northern oysters but heterozygous in southern oysters (S\_het) across 10 chromosomes. **d**, The ratio of genes with non-synonymous SNPs in three oyster populations. Asterisks indicate significant difference (\*\*\*)  $p < 0.001$ .



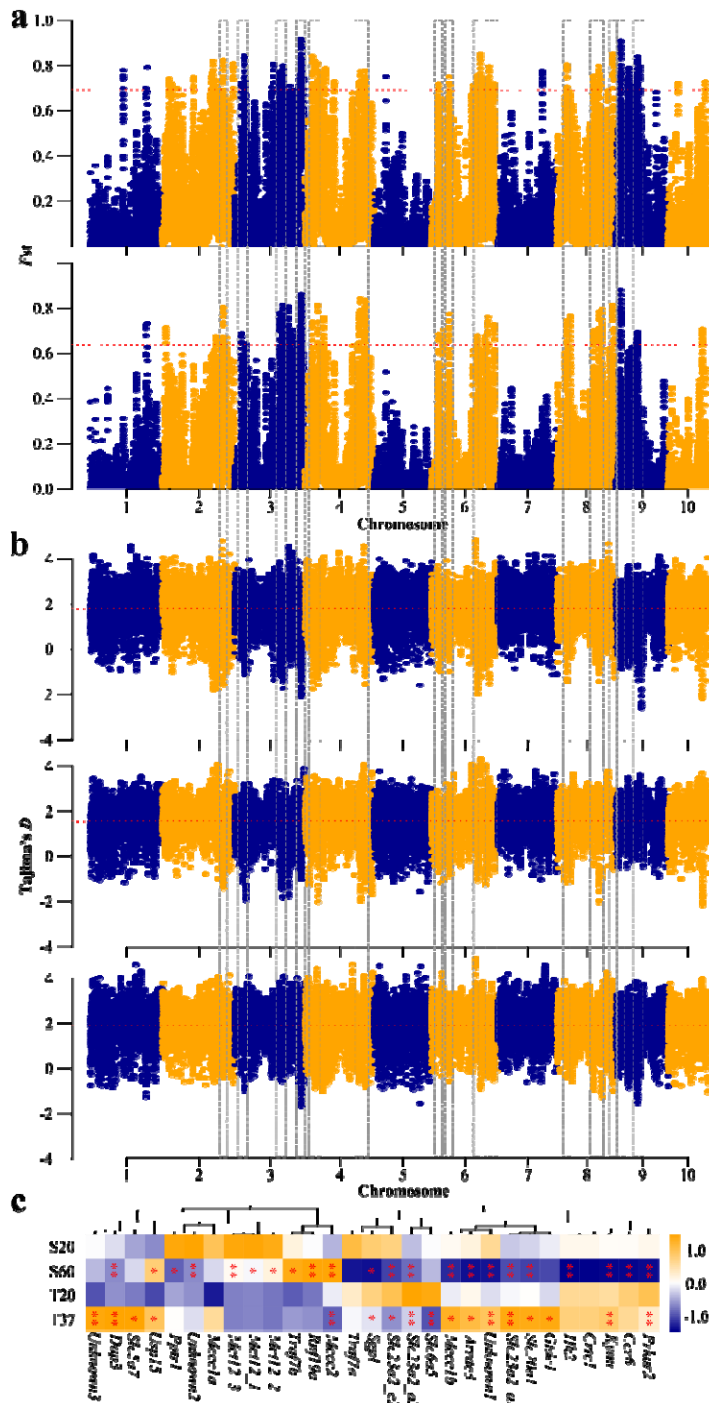


**Fig. 4 | Genome-wide distribution of selective sweep signals and transcriptional responses of selective genes to stresses. a,** Global  $F_{ST}$  values (top 1%, red lines) in two population pairs including northern versus southern (up) and middle versus southern (bottom). **b,** Global Tajima's  $D$  values in northern (up), middle (middle) and southern (bottom) oyster populations. **c,** Expression level of genes under selection in estuarine oysters when exposed to thermal (6 hours under 37 °C) and high-salt (7 days under 60 ‰) conditions. Asterisks indicate significant difference (\*  $p < 0.05$ , \*\*  $p < 0.01$ ).

